Journal of Thermal Analysis, Vol. 32 (1987) 785–795

ON THE DIOXIMINE COMPLEXES OF TRANSITION METALS. LXXVIII[1] TG AND DTA STUDY OF THE THERMAL DECOMPOSITION OF SOME COMPLEXES M[Co(DH)$_2$XY] and [Co(DH)$_2$(H$_2$O)X]

Cs. Várhelyi, J. Zsakó*, G. Liptay*** and *Z. Finta**

*FACULTY OF CHEMICAL TECHNOLOGY, "BABES-BOLYAI" UNIVERSITY, 3400–CLUJ-NAPOCA, ROMANIA
**DEPARTMENT OF INORGANIC CHEMISTRY, TECHNICAL UNIVERSITY, 1521–BUDAPEST, HUNGARY

(Received March 19, 1986)

18 monobasic complex acids of the type H[Co(DH)$_2$XY] (X, Y = Cl, Br, I, NO_2, N_3, NCS, NCSe, CN), or their alkalimetal and ammonium salts, and 5 aquo-acido-nonelectrolytes, [Co(DH)$_2$(H$_2$O)X] (DH = deprotonated dimethylglyoxime), were obtained and their thermal decompositions were studied by means of TG and DTA. The thermolysis processes are discussed. Kinetic parameters have been derived for several decomposition stages and are discussed in terms of the kinetic compensation effect.

The complexes M[Co(DH)$_2$XY] (M = H, K, NH_4; DH = deprotonated dimethylglyoxime; X, Y = Cl, Br, I, NO_2, CN, NCO, NCS, NCSe, N_3) are formed by the oxidation of the components in aqueous-alcoholic solution and by various substitution reactions. The free monobasic acids are moderately strong acids. They are sparingly soluble in water. The best solvents for these compounds are some polar organic solvents (e.g. acetone, DMF, DMSO, alcohols, etc.) [2–13].

I.r. spectral [14] and X-ray investigations have shown that the complex acids of this type have an octahedral trans geometrical configuration. The two dimethylglyoximate monoanions (DH: $C_4H_7N_2O_2$) are situated in the equatorial plane of the octahedral model, stabilized by two very short O—H..O intramolecular hydrogen-bonds. The monodentate ligands X and Y occupy the two free axial coordination sites.

From earlier kinetic studies it is evident that in solution ligand-exchange reactions occur in a wide range of pH, without geometrical transposition.

The thermal decompositions of some complexes [Co(Diox.H)$_2$(amine)$_2$]X (Diox.

John Wiley & Sons, Limited, Chichester
Akadémiai Kiadó, Budapest

H = DH, Dif. H, Niox. H, Heptox. H, Octox. H) have been studied from a kinetic point of view by TG and DTA. The thermal stabilities of these substances were observed to be influenced by the nature of the chelating agent, the amine ligand and the anion X [15–17].

For the above complex acids and their salts, an analogous situation can be expected. Some TG data reported earlier are in agreement with this presumption [18].

In the present paper, 18 acids $H[Co(DH)_2XY]$ and their alkali metal salts, and 5 non-electrolytes $[Co(DH)_2(H_2O)X]$ were obtained and studied by TG and DTA.

Results and discussion

The thermal decompositions of the complexes studied are complicated processes. The TG and DTA curves clearly show the loss of the crystallization water molecules up to 140–180°, the temperature varying with the nature of the cation. Generally, this endothermic process takes place in a single stage, but sometimes in two or even three steps. The main pyrolysis stage (the greatest weight loss in the TG curves) can be observed between 150 and 250°. The DTA curves present a strong maximum in this temperature range. This process presumably corresponds to the oxidation of the dioxime and some X ligands.

Stoichiometric calculations show the weight loss to correspond approximately to the elimination of $DH_2 + HX$, especially when X = Cl, Br or I. With pseudohalides (X = NCS, NCSe and NO_2), the process is more complicated and the TG curves present no well-defined horizontal parts.

Several typical TG and DTA curves are given in Figs 1 and 2.

It is seen that $H[Co(DH)_2Br_2] \cdot 2H_2O$ first loses its crystallization water in a single stage, and the anhydrous acid is then stable up to 200°. Above this temperature a very rapid decomposition occurs, with a large exothermic effect. The analogous acid with X = Y = NCS shows completely different behaviour. Its decomposition begins at much lower temperature, but as a slow process, in several successive stages, none of which correspond to a clear stoichiometry. All these processes are exothermic ones, corresponding to several peaks in the DTA curve.

In the case of $NH_4[Co(DH)_2(NCSe)_2] \cdot 3H_2O$, the loss of the crystallization water occurs in a single endothermic stage and is followed by another endothermic process corresponding to the loss of 0.5 moles of $(NH_4)_2Se$. The further decomposition is a strongly exothermic reaction.

The acid $H[Co(DH)_2(N_3)_2] \cdot H_2O$ loses its crystallization water at relatively high temperature. The decomposition of the complex ion seems to begin as an

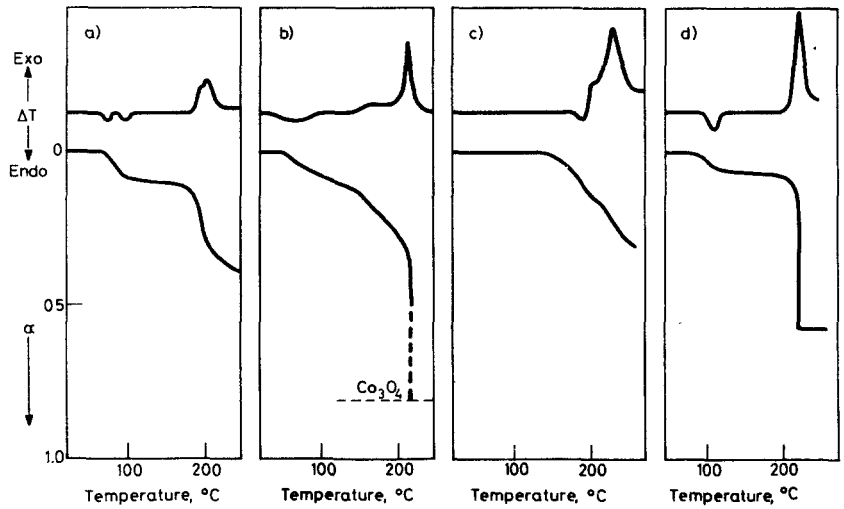

Fig. 1 TG and DTA curves of the complexes a) $H[Co(DH)_2(N_3)Cl]\cdot 2H_2O$; b) $H[Co(DH)_2(NO_2)(CN)]\cdot 2H_2O$; c) $[Co(DH)_2(H_2O)I]$; d) $[Co(DH)_2(H_2O)(NCS)]\cdot 2H_2O$

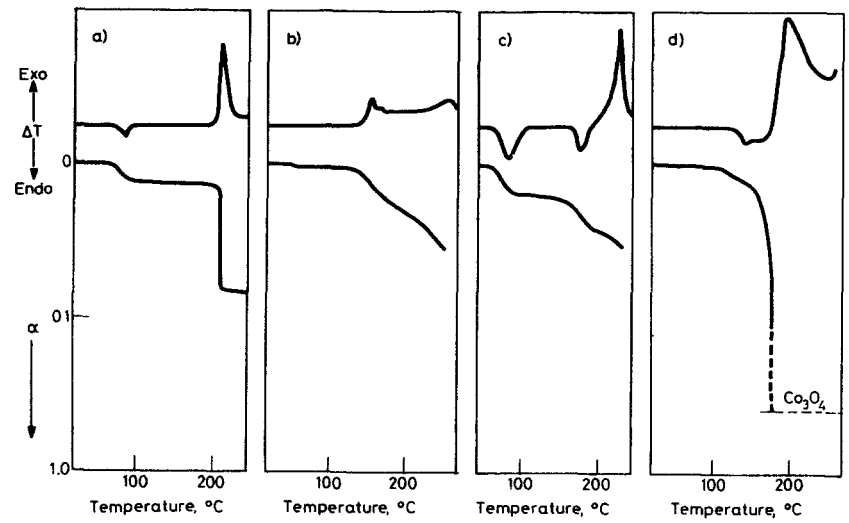

Fig. 2 TG and DTA curves of the complexes: a) $H[Co(DH)_2Br]\cdot 2H_2O$; b) $H[Co(DH)_2(NCS)_2]$; c) $NH_4[Co(DH)_2(NCSe)_2]\cdot 3H_2O$; d) $H[Co(DH)_2(N_3)_2]\cdot H_2O$

endothermic process, which then becomes exothermic and eventually leads to the explosion of the sample. Thus, the final product comprises much less than 19.1%, corresponding to Co_3O_4. It is interesting that if the acid contains only a single N_3 group, a similar explosion is observed with Y = I, but not if Y = Cl.

As seen from Fig. 2, after losing its crystallization water in two successive stages, $H[Co(DH)_2(N_3)Cl] \cdot 2H_2O$ undergoes a relatively slow exothermic decomposition in several successive stages.

Explosions are observed with the NO_2 complexes studied. As an example, the decomposition of $H[Co(DH)_2(NO_2)(CN)] \cdot 2H_2O$ can be seen. After the loss of the crystallization water, slow exothermic processes begin, leading eventually to an explosion.

In the case of the aquo-non-electrolytes, a clear difference is observed between the halogen and the pseudohalogen derivatives. If Y = Br or I, the complex contains no crystallization water, but in the pyrolysis it loses its inner sphere water molecule in an endothermic process, the decomposition further becoming exothermic. On the other hand, with Y = NCS or NCSe, two moles of crystallization water are present, which are lost in a single endothermic stage. The decomposition of the complex itself is exothermic from the beginning. The endothermic effect of the dehydration process is presumably overlapped by the exothermic effect of the other reactions.

The DTA peak temperatures are given in Table 1 for all the complexes studied.

Although the heating rates, q, used were not the same in all cases, several effects of the nature of X and Y upon the position of the first exothermic peak can be observed. Thus, for the acids with X = Y, this temperature increases in the sequence

$$NO_2 < NCS < Cl < Br < I$$

The same sequence is observed for Y in a series containing the same ligand X. In the case of the halogens this order is presumably determined by the strength of the Co-halogen bond, and the lower decomposition temperatures of the NO_2, NCS and NCSe derivatives might be due to the thermal instability of the ligand itself.

On comparison of the first exothermic peak temperatures of the K salts with those of the corresponding acids, an appreciable shift towards higher temperatures is observed in the case of the salts. This effect might be due to the electric charge, but an alternative explanation can also be given. Since the K salts contain an NO_2 group, it might be presumed that, in the dehydration of the free acid, the proton liberated will not be attached to the dimethylglyoxime, through the breaking of a hydrogen-bond, but will be linked to an NO_2 group. This leads to weakening of the Co—N bond and to a shift of the decomposition temperature towards lower temperatures as compared to the situation for the neutral salt, where such a protonation is not possible.

The majority of the thermal curves were recorded in the temperature range

Table 1 DTA peak temperatures at the thermal decomposition of $M[Co(DH)_2XY]\cdot nH_2O$ and $[Co(DH)_2XY]\cdot nH_2O$ type complexes

M	X	Y	n	q deg/min	Endothermic peak temp., °C		Exothermic peak temperature, °C
					external sphere water	complex ion decomposition	
H	Cl	Cl	—	2	—	—	195
H	Br	Br	2	2	84	—	215
H	I	I	—	15	—	—	263
H	NCS	NCS	—	2	—	—	155, 161, 255
H	NCS	Br	—	2	—	—	165
H	NCS	I	—	2	—	—	190, 222
NH_4	NCSe	NCSe	3	3	83	177	235
H	NCSe	Cl	1	15	83	—	179, 252
H	CN	CN	1	3	82	184	235
H	N_3	N_3	1	20	140	165	210
H	N_3	Cl	3	3	75, 92	—	200
H	N_3	I	—	20	—	—	250
H	NO_2	NO_2	1	3	45	—	130, 205
K	NO_2	NO_2	1	10	55	—	240
H	NO_2	Cl	2	3	77, 100, 113	—	160, 202, 243
H	NO_2	I	2	15	88	—	162, 214
H	NO_2	CN	2	3	60	—	177, 217
K	NO_2	CN	1	15	83	—	238
—	H_2O	Br	—	2	—	184	210
—	H_2O	I	—	2	—	183	202, 235
—	H_2O	NO_2	—	2	—	—	190, 238
—	H_2O	NCS	2	2	107	—	230
—	H_2O	NCSe	1	2	115	—	225

between 20° and 300°, and in Table 1 DTA peak temperatures are given only for this interval. In some cases, where the decomposition occurs more slowly, the pyrolysis was followed up to 1000° by using q = 20 deg/min. It was observed that between 400° and 1000° many non-stoichiometric decomposition and oxidation processes take place, with the evolution of CO, CO_2, H_2O, N_2 and NO. The exothermic peaks in the DTA curves prove this presumption. The final product of the thermolysis (with the exception of the chloro and bromo derivatives) is a stoichiometric amount of Co_3O_4, which undergoes transformation into CoO at 925–930°, marked by a strong endothermic peak in the DTA curves.

It is worth mentioning that in the case of several compounds two different heating rates were used. The general picture of the pyrolysis is not affected by the change of the heating rate, but both DTA peaks and TG steps are shifted towards higher temperatures with increasing heating rate.

Table 2 Kinetic parameters of the thermal decomposition of $M[Co(DH)_2XY]\cdot nH_2O$ and $[Co(DH)_2XY]\cdot nH_2O$ type complexes

M	X	Y	n	Loss of crystallization water				Complex decomposition				
				n	E, kJ	$\log Z$	τ^*	n	E, kJ	$\log Z$	τ^*	DTA peak
H	Br	Br	2	0.97	205.0	28.0	2.862	—	—	—	—	—
H	I	I	—	—	—	—	—	3.30	711.6	72.8	2.085	exo
H	NCS	NCS	—	—	—	—	—	1.15	401.1	47.5	2.379	exo
NH_4	NCSe	NCSe	3	1.11	118.9	15.5	2.917	1.30	223.2	23.7	2.268	endo
H	NO_2	NO_2	1	4.88	285.3	47.1	3.283	1.02	159.1	19.8	2.719	exo
K	NO_2	NO_2	1	1.29	49.1	5.1	3.155	—	—	—	—	—
H	N_3	Cl	2	2.05	393.1	57.9	2.918	0.38	203.7	19.8	2.161	exo
				1.33	402.3	56.4	2.792	—	—	—	—	—
H	NO_2	Cl	2	0.77	149.9	21.0	2.964	—	—	—	—	—
H	NO_2	I	2	1.97	261.4	31.2	2.826	—	—	—	—	—
K	NO_2	CN	1	—	—	—	—	1.55	460.5	44.9	2.087	exo
H	NCSe	Cl	1	—	—	—	—	1.18	187.8	22.5	2.516	exo
—	H_2O	NCS	2	0.86	143.0	17.4	2.698	—	—	—	—	—
—	H_2O	I	—	—	—	—	—	0.39	143.7	14.0	2.276	endo
—	H_2O	NO_2	—	—	—	—	—	1.38	320.2	35.3	2.260	exo

Deriving kinetic parameters

In all cases when the TG curve showed a sufficiently clear decomposition stage, an attempt was made to derive kinetic parameters, by using the nomogram method proposed earlier [19]. The apparent kinetic parameters obtained, viz. reaction order n, activation energy E and pre-exponential factor Z, are presented in Table 2. The same Table also contains the reduced position parameter τ^*, meaning $1000/T^*_{0.1}$, where $T^*_{0.1}$ is the temperature at which the transformation degree in the decomposition stage considered would be $\alpha = 0.1$ if the heating rate were 10 deg/min.

As seen from this Table, even for the loss of crystallization water these parameters vary in a rather large interval. It can be observed that the E and $\log Z$ values vary in parallel. Therefore, a $\log Z$ vs. E plot was performed in order to verify the validity of the linear kinetic compensation law

$$\log Z = aE + b$$

The graphical plot showed quite good linearity for all the data presented in Table 2, but the positions of the experimental points suggested a best linearity separately for the loss of crystallization water, and separately for the other decomposition reactions. In order to verify this presumption, the compensation parameters (a and

Table 3 Compensation parameters

	b	a	a'	ϱ
Dehydration + decomposition	−3.20	0.108	0.137	0.943
Dehydration	−2.76	0.152	0.154	0.985
Dehydration*	−2.72	0.148	0.151	0.994
Decomposition	−2.01	0.100	0.121	0.990

* In this variant the point of the acid with X = NO_2, Y = I was omitted

b) were calculated by performing linear regression and by calculating Jaffé's correlation coefficients (ϱ). As seen from Table 3, the linearity is much better if the dehydration reactions are taken separately from the other reactions.

Since the above linear kinetic compensation law results from the Arrhenius equation for an "isokinetic" temperature [20, 21], Table 3 also gives the "theoretical" compensation parameters, denoted by a' and calculated as $a' = \tau^*/2.3R$, i.e. on the presumption that this isokinetic temperature is $T^*_{0.1}$. The a and a' values are seen to be not too far from each other.

In order to obtain a clearer picture, the kinetic parameter values given in Table 2 have been put in the sequence of increasing $T^*_{0.1}$. Further, $T^*_{0.1}$ intervals were determined in which all the E and $\log Z$ values, irrespective of the nature of the process, give a straight line, parameters a and b were derived by means of linear regression. The results are presented in Table 4.

The a values are seen to decrease with decreasing a', without exception, and even the numerical values are very close to each other. This means that there is a rather narrow temperature interval in which the decomposition rates for the different compounds are close to each other. Thus, the parameter a is determined mainly by the decomposition temperature. Nevertheless, under well-standardized working conditions, the variation of the compensation parameter in a series of related compounds may also reveal other effects [21, 22].

Table 4 Compensation parameters as function of $T^*_{0.1}$ interval

$T^*_{0.1}$, °C	a	a'	ϱ
31.6– 69.8	0.160	0.159	0.994
44.0– 76.4	0.153	0.155	1.000
69.7– 94.8	0.151	0.149	0.991
76.4– 97.6	0.149	0.145	0.992
85.2–166.4	0.138	0.134	0.985
124.5–169.5	0.124	0.122	0.993
166.4–189.7	0.122	0.117	0.997
189.7–206.6	0.104	0.110	0.999

Table 5 Analytical data on some $M[Co(DH)_2XY]\cdot nH_2O$ and $[Co(DH)_2XY]\cdot nH_2O$ type complexes

No.	Formula	Mol. weight calcd.	Appearance	Analysis, %		
					calcd.	found
1	$H[Co(DH)_2Cl_2]$	361.05	dark green, brilliant rhomb. plates	Co Cl	16.32 19.64	16.40 19.53
2	$H[Co(DH)_2Br_2]\cdot 2\,H_2O$	485.9	sparkling olive green plates	Co	12.13	12.80
3	$H[Co(DH)_2I_2]$	543.9	green-brown sparkling plates	Co I	10.83 46.67	10.92 46.40
4	$H[Co(DH)_2(NCS)_2]$	406.4	red-brown microcryst.	Co S	14.50 15.78	14.35 15.99
5	$H[Co(DH)_2(NCS)Br]$	428.1	brown microcryst.	Co S	13.77 7.49	13.70 7.70
6	$H[Co(DH)_2(NCS)I]$	475.1	dark brown microcryst.	Co S	12.40 6.75	12.30 6.48
7	$(NH_4)_3[Co(DH)_2(NCSe)_2]\cdot 3\,H_2O$	571.2	brown trigonal prisms	Co N H_2O	10.30 17.16 9.46	10.40 17.10 9.70
8	$H[Co(DH)_2(NCSe)Cl]\cdot H_2O$	448.6	brown microcryst.	Co H_2O	13.14 4.01	13.30 4.30
9	$H[Co(DH)_2(CN)_2]\cdot H_2O$	360.2	yellow sparkling hexagonal plates	Co N H_2O	16.36 23.33 5.00	16.20 23.10 5.40
10	$H[Co(DH)_2(N_3)_2]\cdot H_2O$	392.2	sparkling bown prisms	Co H_2O N	15.02 4.59 35.72	14.88 4.24 35.09
11	$H[Co(DH)_2(N_3)Cl]\cdot 3\,H_2O$	421.6	green rhomb. plates	Co H_2O	13.98 12.81	14.27 12.10
12	$H[Co(DH)_2(N_3)I]$	459.1	brilliant brown irregular plates	Co	12.84	12.44
13	$H[Co(DH)_2(NO_2)_2]\cdot H_2O$	400.1	yellow microcryst	Co N H_2O	14.73 21.00 4.50	14.65 21.22 4.25
14	$K[Co(DH)_2(NO_2)_2]\cdot H_2O$	438.2	yellow prisms	Co N H_2O	13.45 19.18 4.11	13.35 19.00 4.05
15	$H[Co(DH)_2(NO_2)Cl]\cdot 2\,H_2O$	407.6	brilliant, gold-yellow hexagonal plates	Co N	14.46 17.17	14.10 16.90

Table 5 Continued

No.	Formula	Mol. weight calcd.	Appearance	Analysis, %		
					calcd.	found
16	$H[Co(DH)_2(NO_2)I]\cdot 2H_2O$	499	brown microcryst.	Co	11.81	12.30
				N	14.03	14.90
17	$H[Co(DH)_2(NO_2)(CN)]\cdot 2H_2O$	398.2	long yellow needles	Co	14.80	14.20
				N	21.09	20.60
18	$K[Co(DH)_2(NO_2)(CN)]\cdot H_2O$	418.1	light brown thin plates	Co	14.09	14.60
				N	20.08	20.40
19	$[Co(DH)_2(H_2O)Br]$	387.05	green-brown plates	Co	15.22	15.10
				Br	20.60	20.45
20	$[Co(DH)_2(H_2O)I]$	434.05	dark brown microcryst.	Co	13.57	13.60
				I	29.23	29.10
21	$[Co(DH)_2(H_2O)(NO_2)]$	353.1	large, reddish-brown sparkling plates	Co	16.69	16.56
				N	19.83	19.77
22	$[Co(DH)_2(H_2O)(NCS)]\cdot 2H_2O$	401.3	light brown microcryst.	Co	15.03	15.15
				S	7.99	8.10
				H_2O	8.90	8.60
23	$[Co(DH)_2(H_2O)(NCSe)]\cdot H_2O$	430.1	light brown microcryst.	Co	13.70	13.80
				N	16.28	16.40
				H_2O	4.18	4.30

Experimental

Acids $H[Co(DH)_2X_2]$ *(X = Cl, Br, I,* N_3*, CN, NCS, NCSe).* 20 mmoles of CoX_2 (X = Cl, Br, I) or a mixture of $Co(CH_3COO)_2\cdot 4H_2O$ and KX (X = NCS, NCSe, CN) and 40 mmoles of dimethylglyoxime in 150–200 ml 75% methanol was oxidized by air bubbling during 5–6 hours.

After filtration, the brown solutions were treated with an excess of HCl (or HBr) (50–60 ml conc. acid). The crystalline precipitates were filtered off after 30–40 minutes, washed with dil. acid and ether, and dried in the air. The alkalimetal and ammonium salts can be obtained, in some cases, from the oxidized solutions with an excess of alkali metal or ammonium chloride.

$H[Co(DH)_2(NO_2)_2]\cdot H_2O$. 4 g $Na_3[Co(NO_2)_6]$ in 50–60 ml water was treated with 2.3 g dimethylglyoxime in 100 ml water on a water-bath. After evaporation to 1/4 volume, the solution was filtered and treated with an excess of 20% H_2SO_4. The dinitro-acid crystallized from the aqueous solution.

The mixed acids $H[Co(DH)_2X(NO_2)]$, $H[Co(DH)_2X(NCS)]$ and $H[Co(DH)_2X(N_3)]$ were formed on treatment of the corresponding non-electrolytes $[Co(DH)_2(H_2O)Y]$ (Y = NO_2, NCS, N_3) with an excess of HX.

The non-electrolytes $[Co(DH)_2(H_2O)Y]$ were obtained by hydrolysis of the corresponding complex acids in acidic or basic media.

Purification. The crude products were dissolved in alcohol and poured dropwise into 10% HCl solution. The crystalline products were filtered off and washed with a mixture of ether alcohol (10 : 1).

Analysis. The Co content was determined complexometrically after destruction of the samples with conc. H_2SO_4 and some crystals of KNO_3. The halides were determined with $AgNO_3$ after decomposition of the samples with molten KNO_3 + NaOH. Nitrogen was determined gas-volumetrically and the sulphur content as $BaSO_4$.

The complexes obtained, their aspects and their analysis data are presented in Table 5.

The TG and DTA measurements were carried out with a MOM derivatograph. Sample weight: 100–200 mg, heating rate: 2, 3, 15 or 20 deg/min. Atmosphere: static air. Reference material: α-Al_2O_3. Platinum crucible.

References

1 Part LXXVII. J. Zsakó, Cs. Várhelyi, G. Liptay and J. Borbély-Kuszman, J. Thermal Anal., 31 (1986) 285.
2 F. Feigl and H. Rubinstein, Liebigs Ann. Chem., 433 (1923) 183.
3 L. Cambi and L. Coriselli, Gazz. Chim. Ital., 66 (1936) 81.
4 A. V. Ablov, Bull. Soc. Chim. France (5), 7 (1940) 151.
5 A. V. Ablov and G. P. Syrzova, Zhur. Obshchei. Khim., 25 (1955) 1304.
6 Cs. Várhelyi, J. Zsakó and Z. Finta, Monatsh. Chem., 101 (1970) 1013.
7 A. V. Ablov and N. M. Samush, Doklady Akad. Nauk. SSSR, 133 (1960) 1327.
8 Cs. Várhelyi, I. Gănescu and L. Szotyori, Z. Anorg. Allg. Chem., 386 (1971) 232.
9 R. Ripan, Z. Finta and Cs. Várhelyi, Rev. Roumaine Chim., 19 (1974) 37.
10 L. A. Chugaev, Ber. dtsch. chem. Ges., 41 (1908) 2226.
11 A. V. Ablov, Doklady Akad. Nauk SSSR., 97 (2) (1954) 1019.
12 A. V. Ablov and N. M. Samush, Zhur. Neorg. Khim., 3 (1958) 1818.
13 Z. Finta and Cs. Várhelyi, J. Inorg. Nuclear Chem., 36 (1974) 2199.
14 A. Nakahara, Bull. Chem. Soc. Japan, 28 (1955) 207.
15 J. Zsakó, Cs. Várhelyi and E. Kékedy, J. Inorg. Nuclear Chem., 28 (1966) 2637; 32 (1970) 2999.
16 J. Zsakó, E. Kékedy and Cs. Várhelyi, J. Thermal Anal., 1 (1969) 339; Rev. Roumaine Chim., 15 (1970) 865.
17 J. Zsakó and M. Lungu, J. Thermal Anal., 5 (1973) 77.
18 J. Zsakó, Z. Finta and Cs. Várhelyi, Studia Univ. Babeş-Bolyai, Chem., 14 (2) (1969) 145.
19 J. Zsakó, J. Thermal Anal., 15 (1979) 369.
20 P. D. Garn, J. Thermal Anal., 10 (1976) 99.
21 A. J. Lesnikovich and S. V. Levchik, J. Thermal Anal., 30 (1985) 677.
22 J. Zsakó, Cs. Várhelyi, B. Csegedi and J. Zsakó jr., Thermochim. Acta, 45 (1981) 11.

Zusammenfassung — 18 monobasische Komplexsäuren des Typs $H[Co(DH)_2XY]$ X, Y = Cl, Br, I, NO_2, N_3, NCS, NCSe, CN) oder deren Alkalimetall- und Ammoniumsalze und 5 Aquoacido-Nichtelektrolyte $[Co(DH)_2(H_2O)X]$ (DH = deprotoniertes Dimethylglyoxim) wurden hergestellt. Die thermische Zersetzung dieser Verbindungen wurde mittels TG und DTA untersucht. Die Thermolyseprozesse werden diskutiert. Kinetische Parameter wurden für verschiedene Zersetzungsstufen ermittelt und werden in Verbindung mit dem kinetischen Kompensationseffekt diskutiert.

Резюме — С помощью дериватографа изучено термическое разложение восемнадцати синтезированных одноосновных сложных кислот состава $H[Co(ДН)_2XY]$, где ДН =депротонированный диметилглиоксим, а X, Y = Cl, Br, I, NO_2, N_3, NCS, NCSe, CN, или их щелочных и аммониевых солей, а также пяти акво-ацидо-неэлектролитов $[Co(ДН)_2(H_2O)X]$. Обсужден процесс термолиза. Для нескольких стадий установлены кинетические параметры, обсужденные на основе кинетического компенсационного эффекта.